Turbulence Closure for Static and Dynamic Stall in the Transitional Regime

Joachim Hodara
Ph.D. Candidate

School of Aerospace Engineering
Georgia Institute of Technology
Atlanta, Georgia, 30332-0150, USA

Advanced Modeling & Simulation Seminar Series

NASA Ames Research Center
December 8, 2015

CFD has become **widely accepted** for simple flows.
Meanwhile, in the rotorcraft industry...

Massive Separation:

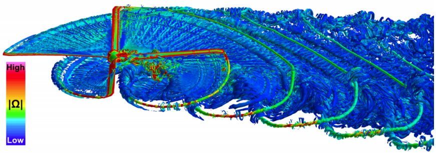

Source: Chaderjian & Ahmad (2012)

Transition to Turbulence:

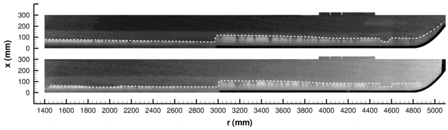

Source: Richter & Schulein (2014)

Still nothing available to **predict both at the same time**.

Turbulence Modeling

Direct Numerical Simulation (DNS)

- All scales resolved
- Very high cost/accuracy

Reynolds-Averaged Navier-Stokes (RANS)

- All scales modeled
- Low cost/accuracy

Large-Eddy Simulation (LES)

- Large scales resolved
- Small scales modeled
- High cost/accuracy

Hybrid RANS-LES

- RANS at walls, LES in separated regions
- Moderate cost / high accuracy

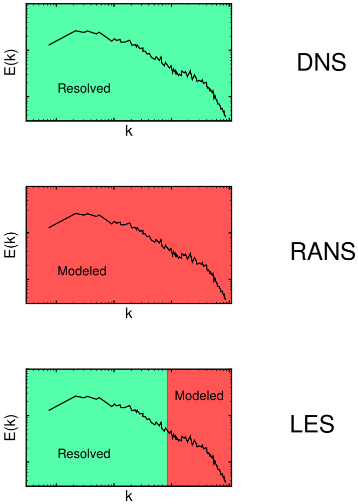

Hybrid RANS-LES Modeling

Detached-Eddy Simulation (DES)[1]

- One model for RANS and LES ($\nu_t \propto Sd^2 \rightarrow S\Delta^2$)
- Good Predictions for massive separation
- Model-Stress-Depletion (MSD) → Delayed/Improved DES[2]

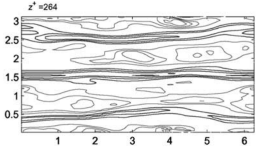

Source: Piomelli et al (2003)

Transfer of momentum in grey zone?

- unphysical flow features
- Need stochastic forcing[3]

Zonal Detached-Eddy Simulation (ZDES)[4]

- User marks RANS and LES regions → reduced MSD
- Less self-sufficient (complex geometry?)

---

[1] Spalart, P.R. (2009). Annu. Rev. Fluid Mech. 41: 181–202.
[2] Spalart, P.R. et al (2006). Theo. Comp. Fluid Dyn. 20(3): 181–195.
[3] Piomelli, U. et al (2003). Int. J. Heat Fluid Fl. 24: 538–550.
[4] Deck, S. (2012). Theor, Comp. Fluid Dyn. 26(6): 523–550.

Additive Hybrid Filter Approach (I)

Rigorous mathematical derivation

Original: $$\frac{\partial\rho}{\partial t} + \frac{\partial\rho u_k}{\partial x_k} = 0$$

Statistical: $$\frac{\partial\dot{\overline{\rho}}}{\partial t} + \frac{\partial\dot{\overline{\rho u_k}}}{\partial x_k} = 0$$

Filtered: $$\frac{\partial\ddot{\overline{\rho}}}{\partial t} + \frac{\partial\ddot{\overline{\rho u_k}}}{\partial x_k} = 0$$

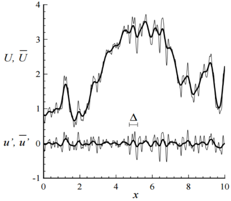

Source: Pope (2000)

RANS rules

$$\dot{\overline{\frac{\partial\phi}{\partial t}}} = \frac{\partial\dot{\overline{\phi}}}{\partial t} \quad ; \quad \dot{\overline{\frac{\partial\phi}{\partial x_i}}} = \frac{\partial\dot{\overline{\phi}}}{\partial x_i} \quad ; \quad \dot{\overline{\dot{\overline{\phi}}}} = \dot{\overline{\phi}}$$

LES rules

$$\ddot{\overline{\frac{\partial\phi}{\partial t}}} = \frac{\partial\ddot{\overline{\phi}}}{\partial t} \quad ; \quad \ddot{\overline{\frac{\partial\phi}{\partial x_i}}} = \frac{\partial\ddot{\overline{\phi}}}{\partial x_i} \quad ; \quad \ddot{\overline{\ddot{\overline{\phi}}}} \neq \ddot{\overline{\phi}}$$

Additive Hybrid Filter[5]: $\overline{\phi} = \mathcal{F}\dot{\overline{\phi}} + (1-\mathcal{F})\ddot{\overline{\phi}}$

Extended to **compressible flows** by Sanchez-Rocha[6]

[5] **Germano, M. (2004). Theor, Comp. Fluid Dyn. 17: 225–331.**

[6] **Sanchez-Rocha, M. and Menon, S. (2009). J. Comput. Phys. 228(6): 2037–2062.**

Additive Hybrid Filter Approach (II)

Hybrid and differentiation operators **do not commute!**

$$\overline{\frac{\partial \phi}{\partial x_k}} = \frac{\partial \overline{\phi}}{\partial x_k} + \frac{\mathcal{F}}{\partial x_k}\left(\ddot{\overline{\phi}} - \dot{\overline{\phi}}\right)$$

We can rigorously derive the **hybrid equations**:

$$\overline{\frac{\partial \rho}{\partial t} + \frac{\partial \rho u_k}{\partial x_k} = 0} \rightarrow \frac{\partial \overline{\rho}}{\partial t} + \frac{\partial \overline{\rho u_k}}{\partial x_k} = \sigma_\rho \neq 0$$

Appearance of **hybrid terms (HT)**: $\sigma_\rho = \frac{\partial \mathcal{F}}{\partial t}\left(\dot{\overline{\rho}} - \ddot{\overline{\rho}}\right) + \frac{\partial \mathcal{F}}{\partial x_k}\left(\dot{\overline{\rho u_k}} - \ddot{\overline{\rho u_k}}\right)$

Need to **reconstruct RANS and LES fields**[7].

So far, **HT ignored** $\rightarrow$ Accurate results for massive separation[8].

[7] **Sanchez-Rocha, M. and Menon, S. (2011). J. Turbul. 12: N16.**

[8] **Shenoy, R. et al (2013). J. Am. Helicopter Soc. 58(3): 1-13.**

Transition Modeling

Method	References	Main issue
DNS	Durbin2007	Cost
LES	Comte1996, Michelassi2003	Cost
e^N Methods	Smith1956, Krumbein2009	Simple cases
Low-Re Models	Jones1973, Biswas1994	Poor predictions
Laminar KE Models	Mayle1997, Walters2002	Poor predictions
Empirical Correlations	Abu-Ghannam1980, Suzen2005	Non-local
$\gamma - Re_\theta$ **Model**	**Langtry2009, Benyahia2012**	**Massive separation**

Correlation-based Transition Model (Fully local)

- Accurate prediction of natural, bypass and separation-induced transitions.
- Implemented in FUN3D, OVERFLOW, elsA, Tau, Fluent, etc.
- Crossflow corrections available
  - Langtry, 2015 (fully local)
  - Grabe and Krumbein, 2014 (non local)
  - Medida and Baeder, 2013 (non local)

Thesis Objectives

There is a **gap in the literature!**

- We can predict separated flows.
- We can predict transitional flows.
- Still nothing to **capture both separation and transition**.

Outline

Objective I: Propose a turbulence closure to fill this gap.

Objective II: Implement the new model in a CFD solver.

Objective III: Evaluate the new model using canonical configurations.

Objective IV: Investigate the model behavior for complex rotorcraft problems.

Objective V: Investigate the effects of the hybrid terms for separated flows.

Design Approach

Approach	**Upsides**	**Downsides**
HRLES	Separation	No transition
$\gamma - Re_\theta$ Model	Transition	Separated flows

We can **extend the HRLES approach to transitional flows**.

RANS Model

- $\gamma - Re_\theta$ Correlation-based Transition Model[9]
- 4 additional PDEs: k, ω, γ, Re_{θ_t}

LES Model

- Localized Dynamic Kinetic Energy Model (LDKM)[10]
- 1 additional PDE: k^{sgs}

Transitional HRLES (tHRLES) Closure

- Captures Transition using RANS model.
- Captures Separation using LES model.

---

[9] **Langtry**, R. and **Menter**, F. (2009). AIAA J. 47(12): 2894-2906.

[10] **Kim**, W. and **Menon**, S. (1999). Int. J. Numer. Meth. Fl. 31(6): 983-1017.

Model Formulation

Four additional PDEs: $\mathcal{K}$, ω, γ, Re_{θ_t}

Hybrid Variables

Hybrid Turbulent Kinetic Energy: $\mathcal{K} = \mathcal{F}k + (1-\mathcal{F})\, k^{sgs}$

Hybrid Eddy Viscosity: $\nu_T = \mathcal{F}\dfrac{a_1\mathcal{K}}{\max(a_1\omega, SF_2)} + (1-\mathcal{F})\, C_\nu \Delta \mathcal{K}^{1/2}$

Equation for the hybrid kinetic energy: $\dfrac{\partial \mathcal{K}}{\partial t} + \dfrac{\partial}{\partial x_j}\left(\bar{\rho}\tilde{u}_j\mathcal{K} - KT_j\right) = KS$

$$KT_j = \mathcal{F}\left[(\mu + \sigma_k\mu_t)\frac{\partial \mathcal{K}}{\partial x_j}\right] + (1-\mathcal{F})\left[\left(\mu + \frac{\mu^{sgs}}{Pr_T}\right)\frac{\partial \mathcal{K}}{\partial x_j}\right]$$

$$KS = \mathcal{F}\left(-\gamma_{eff}\dot{\bar{\tau}}_{ij}\frac{\partial \tilde{u}_i}{\partial x_j} - \overline{\gamma}_{eff}\beta^*\bar{\rho}\omega\mathcal{K}\right) + (1-\mathcal{F})\left(-\ddot{\bar{\tau}}_{ij}\frac{\partial \tilde{u}_i}{\partial x_j} - \bar{\rho}C_\epsilon\frac{\mathcal{K}^{3/2}}{\Delta}\right)$$

The other 3 RANS equations are left unchanged.

Blending Function

Original Blending Function: $\mathcal{F} = F_2 = \tanh\left[\max\left(2\frac{\mathcal{K}^{1/2}}{\beta^*\omega y}; \frac{500\nu}{y^2\omega}\right)^2\right]$

Protect Laminar Boundary Layers

$$\mathcal{F} = \max\left(F_2, F_3\right) \text{ with } F_3 = \exp\left[-\left(\frac{\mathcal{K}^{1/2}y}{120\nu}\right)^2\right]$$

Issue: $\mathcal{F} \to 0$ (LES) in freestream (turb. decay)

Protect Freestream Turbulent Decay

$\mathcal{F} = \max\left(F_2, F_3, F_4\right)$ with

$$F_4 = 1 - \min\left[\max\left(e^{-\left(\frac{y}{c_4\delta}\right)^4}; 1 - \left(\frac{\gamma - 1/c_{e2}}{1 - 1/c_{e2}}\right)^2\right); 1\right]$$

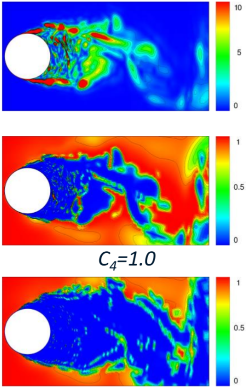

C_4=1.0

C_4=10.0

GTsim

New CFD platform developed at Georgia Tech.

- Rapid implementation of new models.
- Available to international students.

We want a **simple and efficient** code, **targeted for rotorcraft applications**:

- Classic aerodynamics (no reacting flows, low K_n, etc)
- 3D, compressible, unsteady applications.
- Mostly simple geometries → structured topologies.

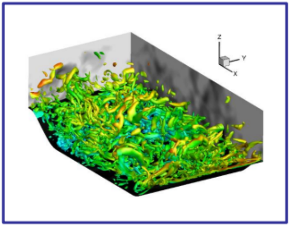

High-Fidelity Simulations

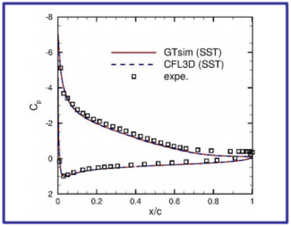

Extensively Validated

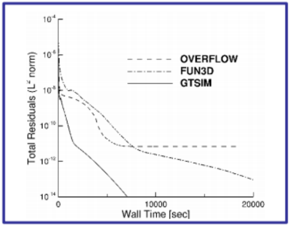

Computationally Efficient

Spatial Discretization

3D, **finite-volume** (cell-centered, structured)

Grid motion capability (rigid translation/rotation with ALE formulation)

Convective Terms

High-Fidelity Turbulent Flows:

- 2nd or 4th order central differences.
- 4th order dissipation (Jameson and Turkel).

High-Speed Flows:

- Central differences with 2nd order dissipation (Jameson).
- Roe's FDS with 3rd order MUSCL reconstruction.
- Multiple slope limiters (Minmod, Superbee, etc).

Transport Terms

- 2nd order central differences.

Temporal Discretization

2nd order **Implicit time marching** (with Dual Time Stepping):

$$\left[\left(\frac{V}{\Delta\tau}+\frac{3V}{2\Delta t}\right)\mathbf{I}-\frac{\partial\mathbf{R}^m}{\partial\mathbf{Q}}\right]\Delta\mathbf{Q}^m=\mathbf{R}^m-V\frac{3\mathbf{Q}^m-4\mathbf{Q}^n+\mathbf{Q}^{n-1}}{2\Delta t}$$

Flux Jacobian: 1st order Steger and warming (inviscid) and TSL (viscous)

Linear Solver: Lower-Upper SSOR $\rightarrow (\mathcal{L}+\mathcal{D})\,\mathcal{D}^{-1}\,(\mathcal{D}+\mathcal{U})\,\Delta\mathbf{Q}^m=\overline{\mathbf{R}}^m$

- Forward sweep: $\Delta\mathbf{Q}^{(p+1/2)}=\mathcal{D}^{-1}\left(\overline{\mathbf{R}}^m-\mathcal{U}\Delta\mathbf{Q}^{(p)}-\mathcal{L}\Delta\mathbf{Q}^{(p+1/2)}\right)$
- backward sweep: $\Delta\mathbf{Q}^{(p+1)}=\mathcal{D}^{-1}\left(\overline{\mathbf{R}}^m-\mathcal{U}\Delta\mathbf{Q}^{(p+1)}-\mathcal{L}\Delta\mathbf{Q}^{(p+1/2)}\right)$

Parallel implementation (MPI) $\rightarrow$ GS sweeps converge to "serial" solution.

Turbulence Modeling

Turbulence model **loosely coupled**.

Treatment of source terms S as suggested by Spalart[11]

$$\mathbf{S}^{m+1} = \mathbf{S}^m + \text{neg}\left(\frac{\partial \mathbf{S}}{\partial \mathbf{Q}}\right) \Delta \mathbf{Q}^m \quad \text{with} \quad \text{neg}(x) = \begin{cases} x & \text{if} \quad x \leq 0 \\ 0 & \text{if} \quad x > 0 \end{cases}$$

Models currently implemented:

- $k - \omega$ SST Model (Menter, 2003)
- $\gamma - Re_\theta$ Transition Model (Langtry, 2009, 2015)
- HRLES (Sanchez-Rocha, 2009)
- DDES (Griskevitch, 2012)
- tHRLES (Hodara, 2015)

[11] **Spalart, P. and Allmaras, S. (1994). Recherche Aerospatiale. 1: 5-21.**

Code Verification

Case	Regime	Model	2D/3D	Results
Flat Plate	Laminar	none	2D	lamFlatPlate
Flat Plate	Turbulent	$k-\omega$ SST	2D	turbFlatPlate
Flat Plate	Transitional	$\gamma - Re_\theta$	2D	tranFlatPlate
Bump in channel	Turbulent	$k-\omega$ SST	2D	bumpChannel
Bump in channel	Turbulent	$k-\omega$ SST	3D	3dbumpChannel
NACA0012	Turbulent	$k-\omega$ SST	2D	turbNaca0012
NACA0012	Turbulent	HRLES	3D	3dNaca0012
NACA4412	Turbulent	$k-\omega$ SST	2D	turbNaca4412
S809	Transitional	$\gamma - Re_\theta$	2D	tranS809
Circular Cylinder	Turbulent	$k-\omega$ SST	2D	turbCylinder
Circular Cylinder	Turbulent	HRLES	3D	3dCylinder
Prolate Spheroid	Transitional	$\gamma - Re_\theta$	3D	tranSpheroid
Swept NLF(2)-0415	Transitional	$\gamma - Re_\theta$	3D	tranNLF20415

Code Performance

Simple Turbulent Flat Plate Case

- Identical machines (4 CPUs).
- Identical grids and conditions.

Numerical Methods

- Similar schemes (2nd order Roe, 2nd order viscous, steady)
- Different convergence schemes (best practices)

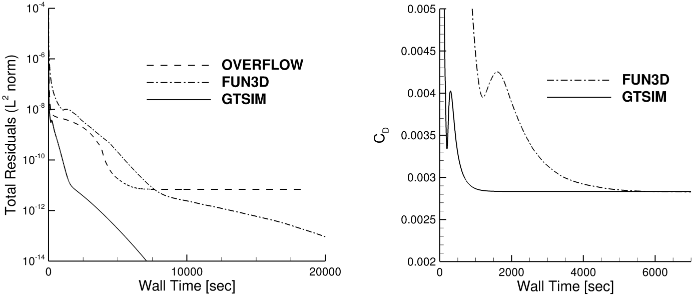

Transitional Flat Plate

Does the model **properly recovers its RANS baseline?**

ERCOFTAC T3 Cases

- H-grid (399 × 50 × 100), $y^+ < 1$.
- Correct turbulent decay.
- Transition captured accurately.

Case	Re_L	Tu [%]
T3A	0.61×10^6	3.3
T3B	1.07×10^6	6.5
T3A-	2.24×10^6	0.874
TSK	5.68×10^6	0.18

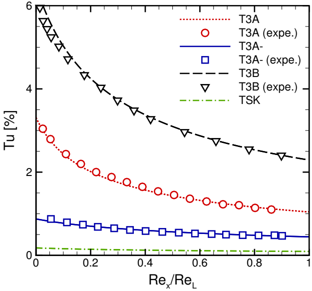

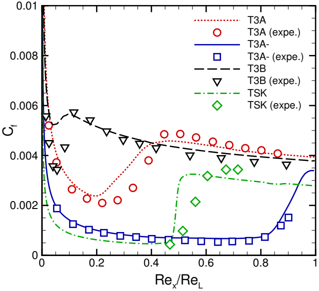

Transitional NACA 64-415 Wing

Slightly more complex case (**pressure gradients**)

Semi-infinite Wing

- C-grid ($897 \times 64 \times 160$), $y^+ < 1$.
- $Re_c = 3 \times 10^6$, $M_\infty = 0.1$.
- $\Delta t \times u_\infty \times c^{-1} = 0.01$ (sub-iterations $\rightarrow$ 2 OM).

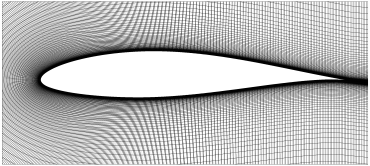

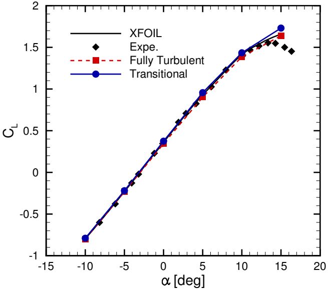

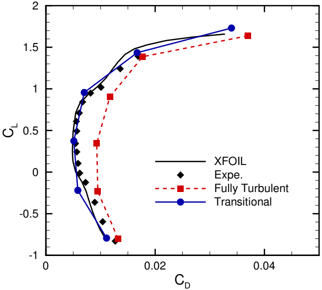

Transitional Circular Cylinder in Crossflow

Test Conditions

- $Re_D = 10 \rightarrow 2 \times 10^6$
- $M_\infty = 0.1$ ($\Delta\rho_{max} < 1.1\%$)
- Natural transition (low turb.)

Expected Physics

- Massive separation
- Drag crisis at $Re_D \sim 10^5$

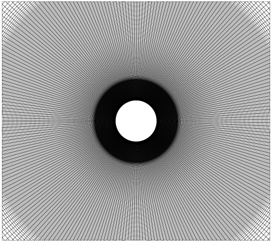

Numerical Methods

- O-grid ($256 \times 128 \times 295$), $y^+ < 1$
- Spanwise width = 2D
- $\Delta t \times u_\infty \times D^{-1} = 0.01$
- sub-iterations $\rightarrow$ 2 OM drop

Turbulence Modeling

URANS

- $k - \omega$ SST (turbulent)
- $\gamma - Re_\theta$ (transitional)

Hybrid RANS-LES

- HRLES (turbulent)
- THRLES (transitional)

Overall Comparison

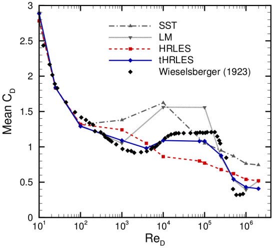

Zoom Drag Plot

Model	Separation	Transition
SST	No	No
LM	No	Yes
HRLES	Yes	No
THRLES	**Yes**	**Yes**

Results at $Re_D = 3,900$

Model	Mean C_D	Strouhal No.	Sep. Angle
SST	1.58	0.238	98.4°
LM	1.35	0.230	96.5°
HRLES	1.05	0.210	88.0°
THRLES	**1.03**	**0.209**	**88.0°**
Expe.[12]	0.99 ± 0.05	0.215 ± 0.005	$86^\circ \pm 2^\circ$

[12] **Son, J.S. et al (1969). J. Fluid Mech. 35(2): 353–368.**

Wake Transition (THRLES)

Observed Physics

- $\mathbf{Re_D < 100}$: 2D steady solution.
- $\mathbf{Re_D \sim 100}$: 2D vortex street (no spanwise variations, laminar).
- $\mathbf{Re_D > 100}$: Wake becomes 3D, still laminar.
- $\mathbf{Re_D > 1,000}$: Wake becomes increasingly turbulent.

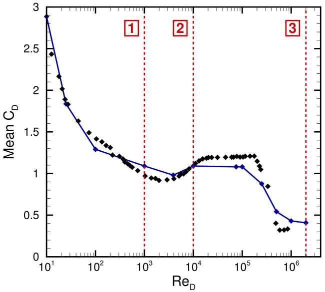

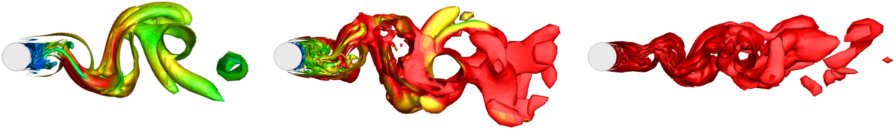

[1] $Re_D = 10^3$ **[2]** $Re_D = 10^4$ **[3]** $Re_D = 2 \times 10^6$

Transition and Separation Locations (THRLES)

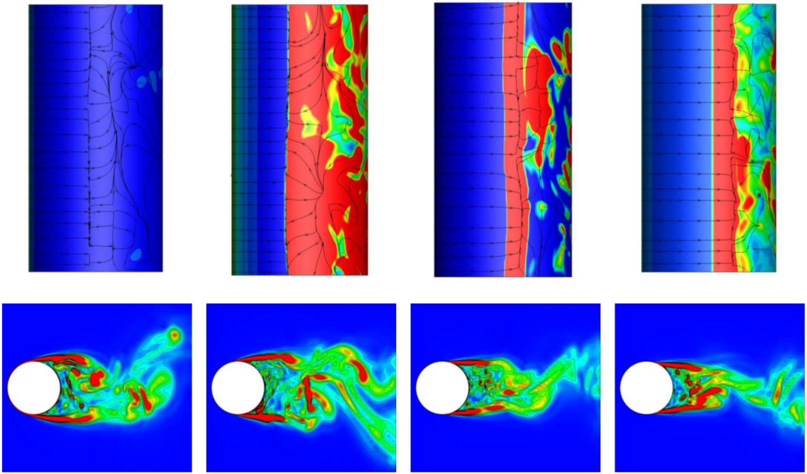

$Re_D = 10^4$ | $Re_D = 2.5 \times 10^5$ | $Re_D = 5 \times 10^5$ | $Re_D = 10^6$

Mean Velocity Profiles (THRLES)

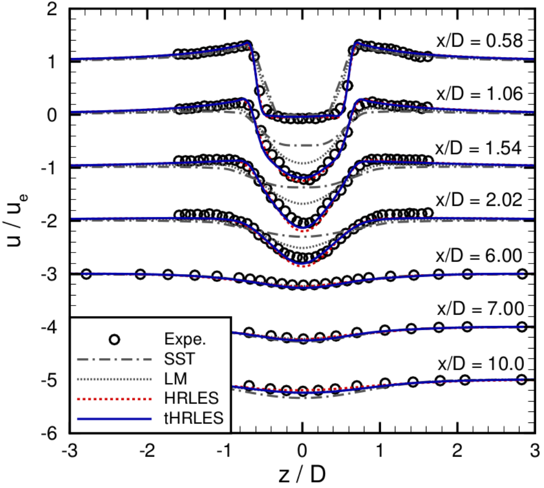

- Expe. at $Re_D = 5,000$[13]
- **URANS very dissipative** (peak 60% lower at 1.06D)
- HRLES and THRLES **within 9%** at 10D

Overall, excellent THRLES results

[13] **Ong**, **L. and Wallace**, **J. (1996). Exp. Fluids 20(6): 441–453**.

Computational Cost

Computational Cost Study

- Large 3D grid.
- Same setup, parameters, inputs, etc.

Turbulence	Exec. Time	Mem. Req.
No Model	1.00	1.00
SST	1.28	1.28
HRLES	1.29	1.31
LM	1.69	1.58
THRLES	1.71	1.69

- Cost driven by number of PDEs.
- **NB:** Algorithm dependent (i.e. spectral radius approx.)

Conclusions

THRLES **cost only slightly higher than LM** (but HRLES constraints!)

Reverse Flow

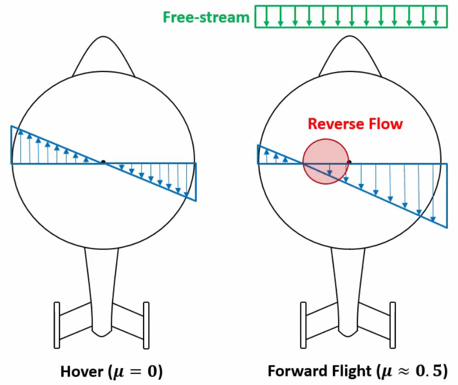

Advance ratio: $\mu = \dfrac{U_\infty}{\Omega R}$

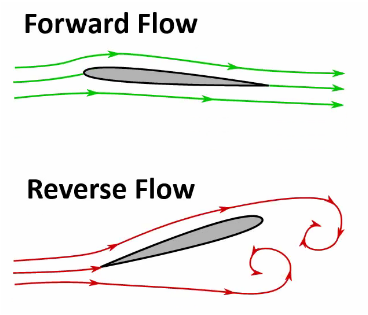

Conventional helicopters **cannot operate at high advance ratios!**

Literature Review

Experimental Investigations:

- **(Datta, 2013):** Full-scale UH-60 $\rightarrow$ Reverse flow responsible for unsteady loads that increase fatigue.
- **(Lind, 2014):** Time-averaged results at $Re_c \sim \mathcal{O}\left(10^5\right)$.
- **(Mayo, 2013):** Time-averaged yawed blades.
- **(Lee, 2012):** Smoke-visualization. Qualitative analysis only.

Numerical Investigations:

- **(harris, 2008):** Comprehensive codes fail for $\mu > 0.6$.
- **(Lee, 2012):** 2D URANS $\rightarrow$ not sufficient (vortex shedding).
- **(Smith, 2011):** Blind CFD (3D unsteady, HRLES). Good results, but only analyzed time-averaged forces.

Conclusions

- No **time-accurate analysis** of airfoils in reverse flow.
- **Need better understanding** to develop analytic models.

Numerical Methods

Test Conditions

- Collaboration with Prof. Jones and Andrew Lind at UMD.
- Static and dynamically pitching NACA0012 airfoil.
- $Re_c \sim \mathcal{O}\left(10^5\right)$, incompressible.

Grid-Independence Study (2D, SST)

- $Re_c = 1.1 \times 10^5$, $\alpha = 150°$.
- 50 nodes in boundary layer, $y^+ < 1$.

Grid Level	$\overline{C_L}$	$\overline{C_D}$	St_d
Medium	-1.75	1.19	0.103
Fine	**-1.90**	**1.26**	**0.120**
Very Fine	-1.91	1.27	0.118

- **Final grid:** $999 \times 61 \times 201$.

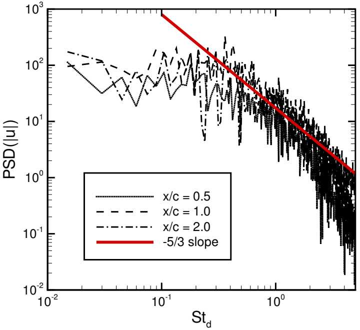

Reverse Flow Regimes

Three reverse flow regimes observed

- Slender body vortex shedding regime.
- Turbulent wake regime.
- Deep stall regime.

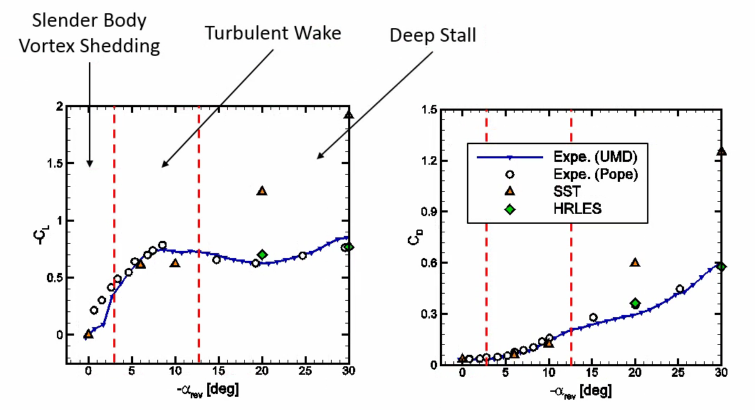

Slender Body Vortex Shedding Regime

Range of conditions

- $-\alpha_{\text{rev}} < 2^\circ$ (at $Re_c = 1.1 \times 10^5$)

Flow Physics

- Boundary layer mostly attached.
- Separation near trailing edge.
- Von Karman vortex street.
- C_D twice the forward flight value.

CFD guidelines

- URANS sufficient.
- C_D within 3%.
- St_d within 13%.

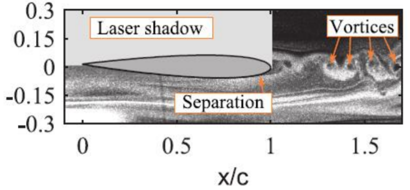

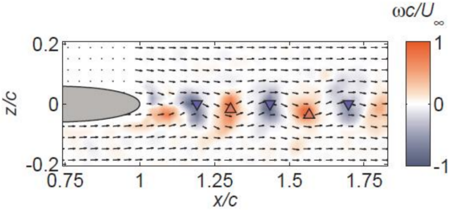

Turbulent Wake Regime

Range of conditions

- $2^\circ < -\alpha_{\text{rev}} < 12^\circ$ (at $Re_c = 1.1 \times 10^5$)

Flow Physics

- Separation at leading-edge.
- Reattachment at mid-chord.
  - Steady for $3^\circ < -\alpha_{\text{rev}} < 6^\circ$
  - Unsteady for $7^\circ < -\alpha_{\text{rev}} < 9^\circ$
- No reattachment for $-\alpha_{\text{rev}} > 10^\circ$.
- Turbulent wake.

CFD guidelines

- URANS sufficient.
- C_D within 7%.
- Steady wake.

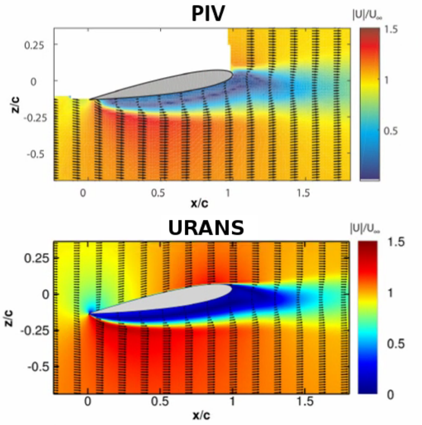

Deep Stall Vortex Shedding Regime

Range of conditions

- $-\alpha_{\text{rev}} > 12^\circ$ (at $Re_c = 1.1 \times 10^5$)

Flow Physics

- Massive separation.
- Large unsteady effects.

CFD guidelines

- URANS not sufficient!
  - C_D within 126%
- HRLES required!
  - C_D within 2%
- Excellent CFD/Expe. agreement.

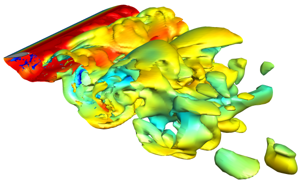

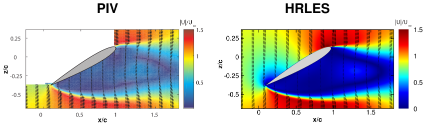

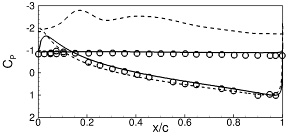

Results at $-\alpha_{rev} = 30^\circ$

Deep Stall Vortex Shedding Regime

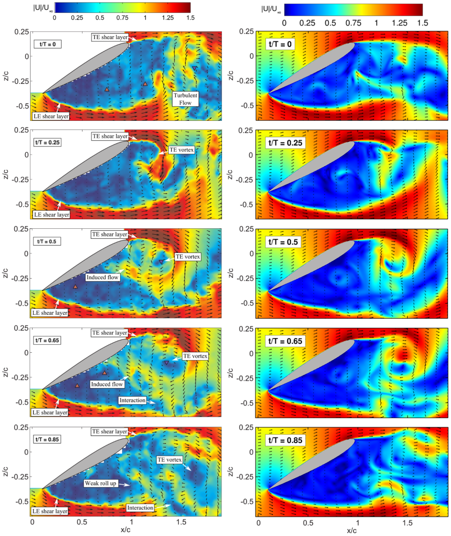

$t/T = 0$

- Well defined shear layer at leading and trailing edges

$t/T = 0.25$

- Trailing edge shear layer rolls up

$t/T = 0.5$

- Formation of a clock-wise vortex
- Induced flow that impinges on the airfoil ($\rightarrow$ unsteady airloads)

$t/T = 0.65$

- Vortex interacts with leading edge shear layer (opposing vorticities)

$t/T = 0.85$

- Vortex and shear layer break down
- Turbulent wake

Dynamic Stall in Reverse Flow

Test Conditions

- $k = 0.16$, incompressible
- $Re_c = 1.65 \times 10^5$
- $-\alpha_{\mathrm{rev}} = 10^\circ \pm 10^\circ$

Numerical Methods

- HRLES closure.
- Temporal resolution study
  - 50,000 time steps / cycle
  - sub-iterations $\rightarrow$ 3OM drop
- Identical kinematics CFD/Exp.
  - Truncated Fourier series
  - 2 modes $\rightarrow \Delta\alpha_{\mathrm{rev}} < 0.07^\circ$

Results

- Five stages of reverse flow
- Good agreement CFD/Expe.

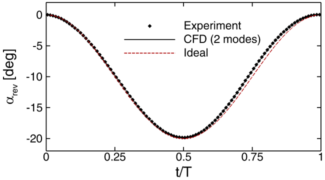

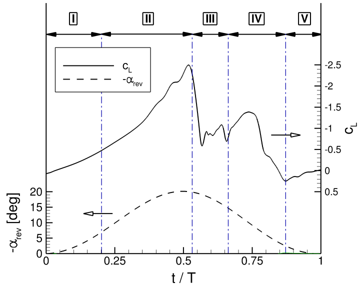

Comparison CFD/Experiments (I)

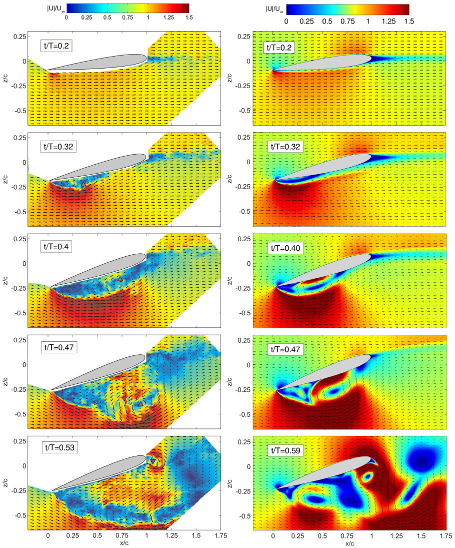

Stage 1

- At $t/T = 0.20$, boundary layer mostly attached.

Stage 2

- At $t/T = 0.32$, boundary layer separates at leading edge, reattaches at mid-chord.
- At $t/T = 0.40$, boundary layer separated. Dynamic vortex convects downstream, induces high velocity (suction) at wall. Phase lag CFD/Exp.
- At $t/T = 0.47$, dynamic vortex moves away from wall. Stronger in CFD.

Stage 3

- At $t/T = 0.53$, primary dynamic vortex entrains trailing edge shear layer $\rightarrow$ vortex (stronger in CFD).

Comparison CFD/Experiments (II)

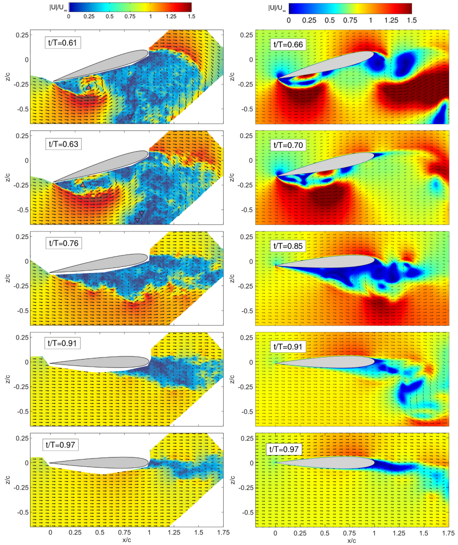

Stage 4

- At t/T = 0.61, secondary dynamic vortex at leading edge. Phase lag CFD/exp.
- At t/T = 0.63, secondary dynamic vortex convects downstream and diffuses.

Stage 5

- At t/T = 0.76, secondary dynamic vortex dissipated → Turbulent wake.
- At t/T = 0.91, boundary layer reattaches (separates at mid-chord).
- At t/T = 0.97, boundary layer separates close to trailing edge.

THRLES predictions

On-going Work...

What to expect?

- Little influence of transition (separation at leading-edge).
- High turbulence levels in the wind tunnel (2-3%).

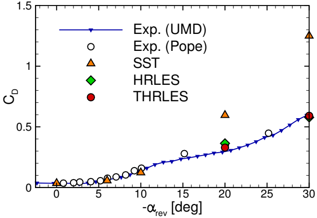

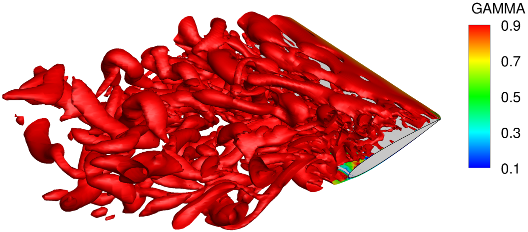

Dynamic simulation coming soon...

Theoretical Background

We can rigorously derive the **hybrid equations**:

$$\overline{\frac{\partial \rho}{\partial t} + \frac{\partial \rho u_k}{\partial x_k} = 0} \rightarrow \frac{\partial \overline{\rho}}{\partial t} + \frac{\partial \overline{\rho u_k}}{\partial x_k} = \sigma_\rho \neq 0$$

Appearance of **hybrid terms (HT)**: $\sigma_\rho = \frac{\partial \mathcal{F}}{\partial t}\left(\dot{\overline{\rho}} - \ddot{\overline{\rho}}\right) + \frac{\partial \mathcal{F}}{\partial x_k}\left(\dot{\overline{\rho u_k}} - \ddot{\overline{\rho u_k}}\right)$

Complete Hybrid Terms

Neglected so far → Very good results, but...

- **Transfer of momentum** in grey zone?[14]
- HT only tested on **flat plates** and **channel flows**.[15]

Conclusions

- Need to investigate **HT for separated flows**.

[14] Sanchez-Rocha, M. and Menon, S. (2009). J. Comput. Phys. 228(6): 2037–2062.

[15] Rajamani, B. and Kim, J. (2010). Flow, Turbul. Combust. 85(3-4): 421-441.

Numerical Implementation

RANS Reconstruction: $\dot{\overline{\phi}} = \dot{\overline{\overline{\phi}}}$

LES Reconstruction:

- Inverse filtering: $\ddot{\overline{\phi}} = \dfrac{\overline{\phi} - \mathcal{F}\dot{\overline{\phi}}}{1 - \mathcal{F}} \rightarrow$ Not stable[16]
- Order of magnitude approximation[17]: $\ddot{\overline{\phi}} = \overline{\phi} + G_{(0,1)} RMS\left(\phi^{\overline{\prime}^R}\right)$

with $RMS\left(\phi^{\overline{\prime}^R}\right) = \sqrt{\dot{\overline{\overline{\phi}\,\overline{\phi}}} - \dot{\overline{\overline{\phi}}}\,\overline{\overline{\phi}}}$

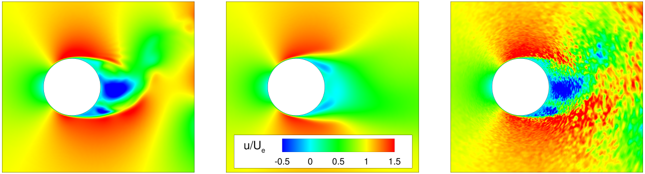

Hybrid RANS LES

[16] Rajamani, B. and Kim, J. (2010). Flow, Turbul. Combust. 85(3-4): 421-441.

[17] Sanchez-Rocha, M. and Menon, S. (2011). J. Turb. 12(16): 1-22.

Periodic Hills

Numerical Methods

- Grid: $(197 \times 187 \times 129)$, $y^+ < 1$
- 4th Order CD ($k_4 = 1/256$)
- Driving body force $\rightarrow Re_b = 10,595$

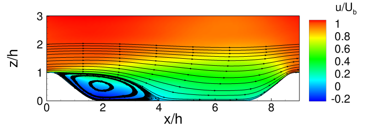

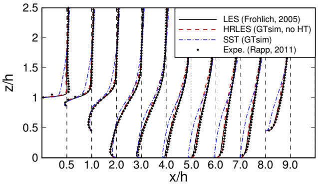

Zoom on graph

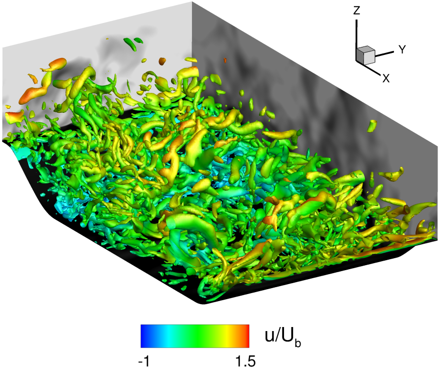

On-going Investigation

- HT for separated flows
- Comparison HRLES/DES

Robin Mod-7 Fuselage

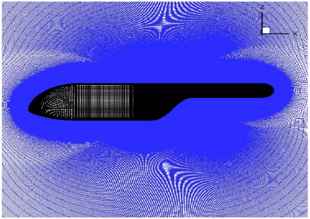

- $M_\infty = 0.1$, $Re = 1.6 \times 10^6$, $\alpha = 0^\circ$
- **Grid sensitivity analysis** $\rightarrow$ 25M cells
- Complex real-life application (THRLES)
- Transitional effects?

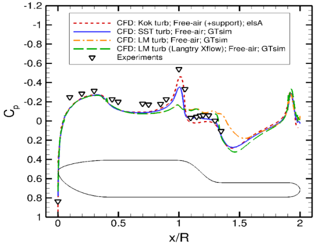

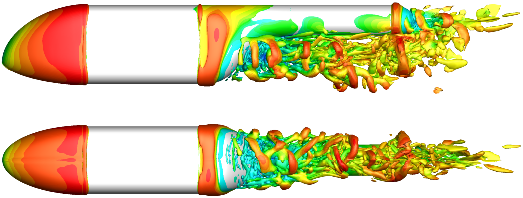

- **On-going work...**

Conclusions

- New THRLES proposed $\rightarrow$ **captures transition AND separation**.
- **High-fidelity CFD platform** developed from scratch.
- Model implemented and verified using:
  - Simple flows: flat plates, wing at moderate incidence.
  - Circular cylinder at $Re_D = 10 \rightarrow 2 \times 10^6$.
- Model successfully applied to **wings in reverse flows**.
- Currently investigating **hybrid terms for separated flows**.

Further Work

Before graduation

- Dynamically pitching airfoil in reverse flow (THRLES)
- Periodic hills with DDES and HRLES+HT.
- Computational cost of HT.

Premature optimization is the root of all evil.

Dr. Donald Knuth

Future Work

- Improved blending function.
- Implementation in FUN3d / OVERFLOW / etc.
- Sustaining freestream turbulence for $\gamma - Re_\theta$.
- More Testing!

Publications

Hodara J., Cross P. and Smith M.J., "Evaluation of Crossflow Transition Models for Rotorcraft Applications, *72nd American Helicopter Society Forum*, Paper 2016-265, West Palm Beach, FL (2016)

Hodara J., Cross P.A. and Smith M.J., "Improved Turbulence and Transition Closures for Separated Flows, *41st European Rotorcraft Forum*, Paper 2015-113, Munich, Germany (2015).

Hodara J., Lind A.H., Jones A.R. and Smith M.J., "Collaborative Investigation of the Aerodynamic Behavior of Airfoils in Reverse Flow, *71st American Helicopter Society Forum*, Paper 2015-267, Virginia Beach, VA (2015)
Best Paper Award (Aerodynamics) - Accepted in JAHS

Jones A.R., **Hodara J.**, Smith M.J., Granlund K., Mulleners K. and Ol M., "Blade Sections in Streamwise Oscillations into Reverse Flow, *71st American Helicopter Society Forum*, Paper 2015-183, Virginia Beach, VA (2015)

Hodara J. and Smith M.J., "Improvement of Crossflow Aerodynamic Predictions for Forward Flight at All Advance Ratios, *40th European Rotorcraft Forum*, Paper 2014-104, Southampton, UK (2014)

Acknowledgments

The investigations were supported by the **U.S. Army/Navy/NASA Vertical Lift Rotorcraft Center of Excellence** at Georgia Institute of Technology under Task 3, under the direction of **Dr. Mahendra Bhagwat** of AFDD, Agreement No. W911W6-11-2-0010. This research is also funded through an **Army Research Office** project under grant number W911NF-13-1-0244, Technical Monitor **Dr. Matthew Munson**.

The author thanks his advisor, **Professor Marilyn Smith**, as well as **Professor Suresh Menon** from Georgia Tech, for access to his high performance computers.

Questions?

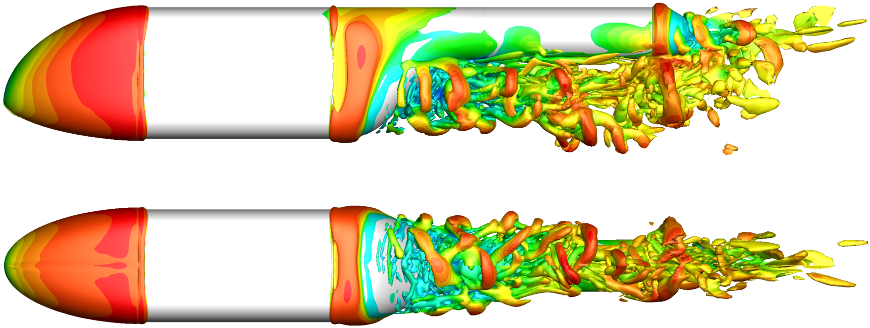

Two-Dimensional Laminar Flat Plate

Test Conditions

$Re_L = 10,000$
$M_\infty = 0.2$
Laminar Flow

Numerical Methods

Grid: 161 $\times$ 65 (130 on plate)
Spatial: 2nd order Roe's FDS
Temporal: Steady solution

Results: (Blasius' Solution)

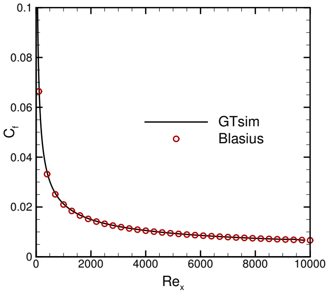

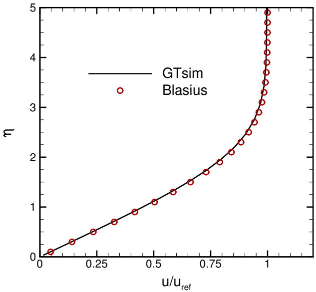

Go Back

Two-Dimensional Turbulent Flat Plate

Test Conditions

$Re_L = 5 \times 10^6$
$M_\infty = 0.2$
Turbulent Flow ($k - \omega$ SST)

Numerical Methods

Grid: Up to 545×385
Spatial: 2nd order Roe's FDS
Temporal: Steady solution

Results: (Turbulence Model Benchmarking Working Group, NASA Langley)

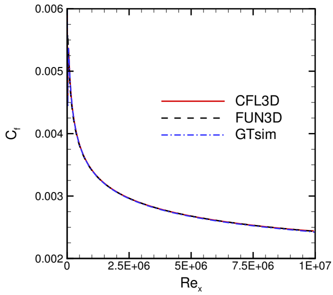

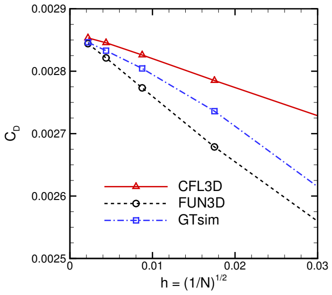

Go Back

Two-Dimensional Transitional Flat Plate

Test Conditions

$Re_L = 0.36 - 3.34 \times 10^6$
$M_\infty = 0.1$
Transitional Flow ($\gamma - Re_\theta$)

Numerical Methods

Grid: 153×100 (124 on plate)
Spatial: 2nd order Roe's FDS
Temporal: Steady solution

Results: (ERCOFTAC T3 Series: Pironneau, 2008)

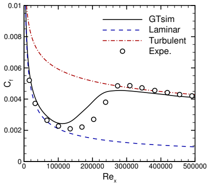

T3A

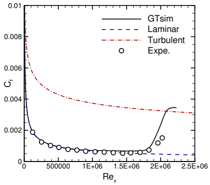

T3A-

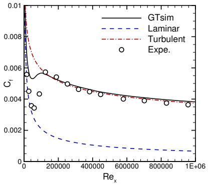

T3B

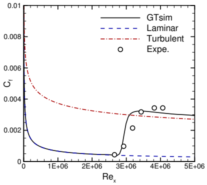

TSK

Go Back

Two-Dimensional Turbulent Bump in Channel

Test Conditions

$Re_L = 3 \times 10^6$
$M_\infty = 0.2$
Turbulent Flow ($k - \omega$ SST)

Numerical Methods

Grid: 177×81 (coarse)
Spatial: 2nd order Roe's FDS
Temporal: Steady solution

Results: (Turbulence Model Benchmarking Working Group, NASA Langley)

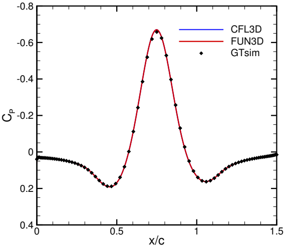

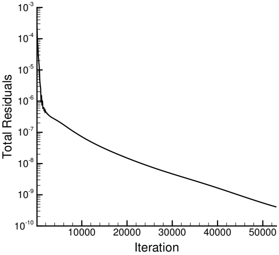

Code	C_D
CFL3D	0.00368
GTsim	0.00382

Go Back

Three-Dimensional Turbulent Bump in Channel

Test Conditions

$Re_L = 3 \times 10^6$
$M_\infty = 0.2$
Turbulent Flow ($k - \omega$ SST)

Numerical Methods

Grid: $33 \times 353 \times 161$
Spatial: 2nd order Roe's FDS
Temporal: Steady solution

Results: (Turbulence Model Benchmarking Working Group, NASA Langley)

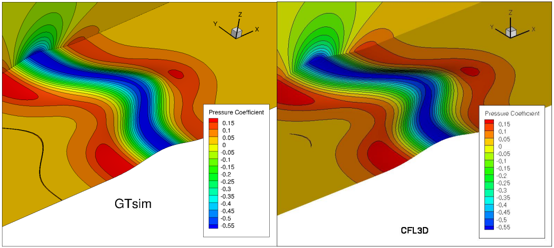

Code	C_D
CFL3D	0.00364
FUN3D	0.00361
GTsim	0.00362

Go Back

Two-Dimensional Turbulent NACA0012 Airfoil

Test Conditions

$Re_c = 6 \times 10^6$
$M_\infty = 0.15$
Turbulent Flow ($k - \omega$ SST)

Numerical Methods

Grid: 897 $\times$ 257 (C-grid)
Spatial: 2nd order Roe's FDS
Temporal: Steady solution

Results: (Turbulence Model Benchmarking Working Group, NASA Langley)

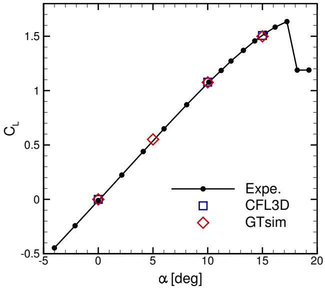

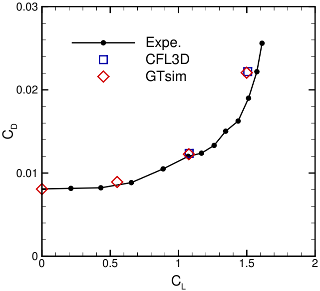

Go Back

Three-Dimensional Turbulent NACA0012 Airfoil

Test Conditions

$Re_c = 100,000$
$M_\infty = 0.2$
Turbulent Flow (SST/HRLES)

Numerical Methods

Grid: $499 \times 31 \times 161$ (O-grid)
Spatial: 2nd order Roe's FDS
Temporal: 5,000 steps/cycle

Results: (Strelets, 2001)

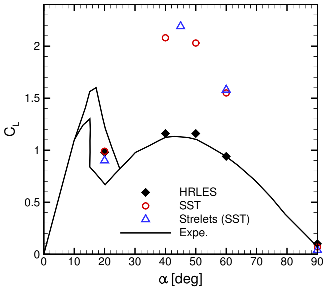

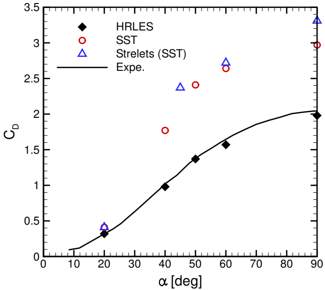

Go Back

Two-Dimensional Turbulent NACA4412 Airfoil

Test Conditions

$Re_c = 1.52 \times 10^6$
$M_\infty = 0.09$, $\alpha = 13.87°$
Turbulent Flow ($k - \omega$ SST)

Numerical Methods

Grid: 481 × 253 (O-grid)
Spatial: 2nd order Roe's FDS
Temporal: Steady solution

Results: (Turbulence Model Benchmarking Working Group, NASA Langley)

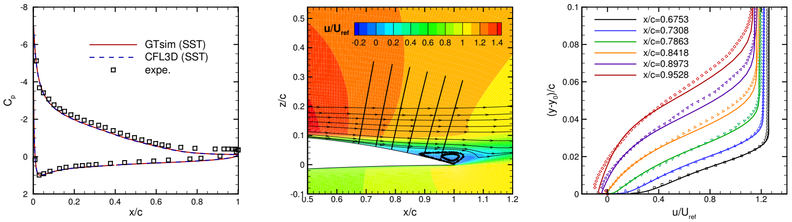

Go Back

Two-Dimensional Transitional S809 Airfoil

Test Conditions

$Re_c = 2 \times 10^6$
$M_\infty = 0.1$
Transitional Flow ($\gamma - Re_\theta$)

Numerical Methods

Grid: 918×161 (O-grid)
Spatial: 2nd order Roe's FDS
Temporal: Steady solution

Results: (Somers, 1981 - Langtry, 2006)

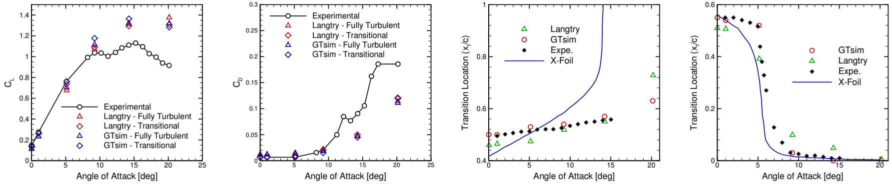

Go Back

Two-Dimensional Turbulent Circular Cylinder

Test Conditions

$Re_D = 10,000$
$M_\infty = 0.2$
Turbulent Flow ($k - \omega$ SST)

Numerical Methods

Grid: 129 $\times$ 81 (O-grid)
Spatial: 2nd order Roe's FDS
Temporal: Convergence study

Results: (CFL3D Documentation)

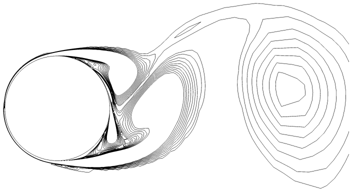

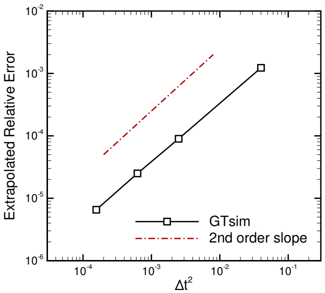

Go Back

Three-Dimensional Turbulent Circular Cylinder

Test Conditions

$Re_D = 3,900$
$M_\infty = 0.2$
Turbulent Flow (SST/HRLES)

Numerical Methods

Grid: 136 × 48 × 144 (O-grid)
Spatial: 2nd order Roe's FDS
Temporal: 1000 steps/cycle

Results: (Beaudan, 1994 - Son, 1969 - Ong, 1996)

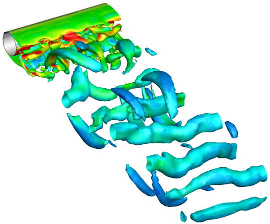

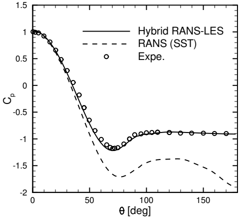

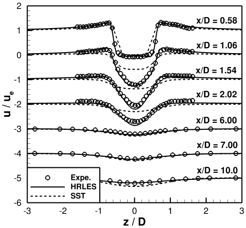

Go Back

Three-Dimensional Transitional Prolate Spheroid

Test Conditions

$Re_L = 6.5 \times 10^6$
$M_\infty = 0.292$, $\alpha = 15°$
Transitional Flow (Langtry XFlow)

Numerical Methods

Grid: $300 \times 73 \times 201$
Spatial: 2nd order Roe's FDS
Temporal: steady solution

Results: (Langtry, 2015)

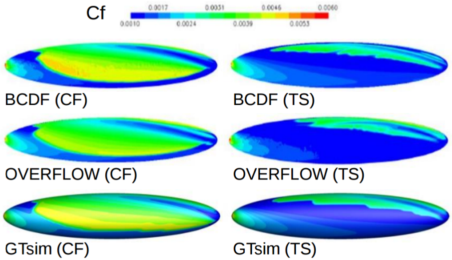

Go Back

Infinite Transitional Swept NLF(2)-0415 Wing

Test Conditions

$Re_L = 2.19 - 3.73 \times 10^6$
$M_\infty = 0.292$, $\alpha = -4°$, $\Lambda = 45°$
Transitional Flow (Langtry XFlow)

Numerical Methods

Grid: $797 \times 100 \times 100$
Spatial: 2nd order Roe's FDS
Temporal: steady solution

Results: (Sa, 2015)

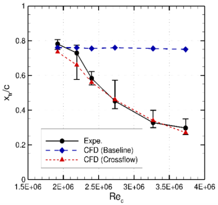

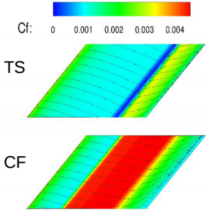

Go Back

Circular Cylinder - Drag Plot

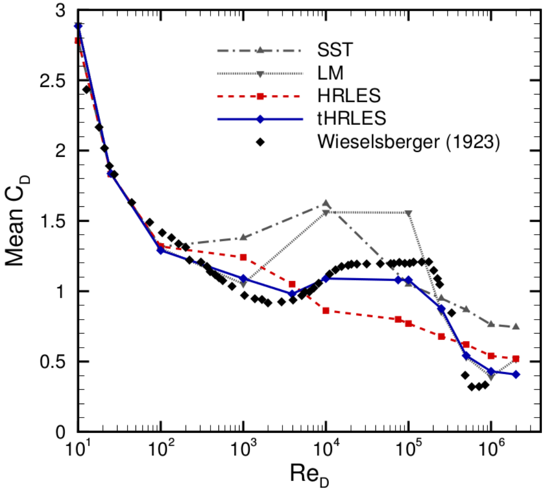

Go Back

Incompressible Hybrid Terms (Stat.)

$$\sigma_\rho = \frac{\partial \mathcal{F}}{\partial x_j}\left[\dot{\overline{\rho}}\dot{\tilde{u}}_j - \ddot{\overline{\rho}}\ddot{\tilde{u}}_j\right]$$

$$\begin{aligned}\sigma_{\rho u_i} = \frac{\partial \mathcal{F}}{\partial x_j}&\left[\dot{\overline{\rho}}\dot{\tilde{u}}_i\dot{\tilde{u}}_j - \ddot{\overline{\rho}}\ddot{\tilde{u}}_i\ddot{\tilde{u}}_j + \dot{\overline{\tau}}\left(u_i, u_j\right) - \ddot{\overline{\tau}}\left(u_i, u_j\right) + \left(\dot{\overline{p}} - \ddot{\overline{p}}\right)\delta_{ij} - \left(\dot{\tilde{\tau}}_{ij} - \ddot{\tilde{\tau}}_{ij}\right)\right] \\ &- \frac{\partial}{\partial x_j}\mu\left[\frac{\partial \mathcal{F}}{\partial x_j}\left(\dot{\tilde{u}}_i - \ddot{\tilde{u}}_i\right) + \frac{\partial \mathcal{F}}{\partial x_i}\left(\dot{\tilde{u}}_j - \ddot{\tilde{u}}_j\right) + \frac{2}{3}\frac{\partial \mathcal{F}}{\partial x_k}\left(\dot{\widetilde{u_k}} - \ddot{\widetilde{u_k}}\right)\delta_{ij}\right]\end{aligned}$$

$$\begin{aligned}\sigma_{\rho E} = \frac{\partial \mathcal{F}}{\partial x_j}&\left[\dot{\overline{\rho}}\dot{\tilde{E}}\dot{\tilde{u}}_j - \ddot{\overline{\rho}}\ddot{\tilde{E}}\ddot{\tilde{u}}_j + \dot{\overline{\tau}}\left(E, u_j\right) - \ddot{\overline{\tau}}\left(E, u_j\right)\right. \\ &+ \dot{\tilde{u}}_j\dot{\overline{p}} - \ddot{\tilde{u}}_j\ddot{\overline{p}} + \dot{\overline{\tau}}\left(u_j, p\right) - \ddot{\overline{\tau}}\left(u_j, p\right) + \\ &-\kappa\left(\frac{\partial \dot{\tilde{T}}}{\partial x_j} - \frac{\partial \ddot{\tilde{T}}}{\partial x_j}\right) - \dot{\overline{\tau}}\left(\frac{\partial T}{\partial x_j}, \kappa\right) + \ddot{\overline{\tau}}\left(\frac{\partial T}{\partial x_j}, \kappa\right) \\ &\left. - \left(\dot{\tilde{\tau}}_{ij}\dot{\tilde{u}}_i - \ddot{\tilde{\tau}}_{ij}\ddot{\tilde{u}}_i\right) - \dot{\overline{\tau}}\left(\tau_{ij}, u_i\right) + \ddot{\overline{\tau}}\left(\tau_{ij}, u_i\right)\right]\end{aligned}$$

Go Back

Periodic Hills - Mean Velocity Profiles

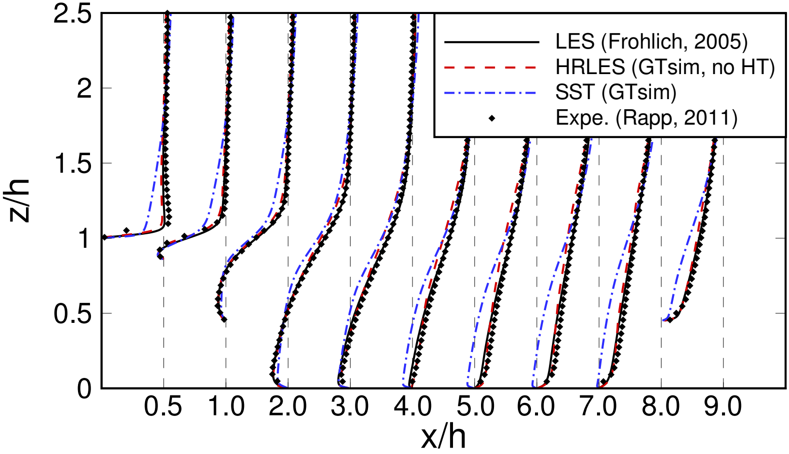

Go Back